



A long range distal enhancer controls temporal fine-tuning of *PAX6* expression in neuronal precursors

Marine Lacomme^{a,b}, François Medevielle^a, Henri-Marc Bourbon^a, Elodie Thierion^c, Dirk-Jan Kleinjan^d, Mélanie Roussat^a, Fabienne Pituello^a, Sophie Bel-Vialar^{a,*}

^a Centre de Biologie du Développement (CBD), Centre de Biologie Intégrative (CBI), Université de Toulouse, CNRS, UPS, France

^b Cellular Neurobiology Research Unit, Institut de recherches cliniques de Montréal (IRCM), Montreal, Québec, Canada

^c Cancer Research UK Cambridge Institute, University of Cambridge, Cambridge, United Kingdom

^d IUK Centre for Mammalian Synthetic Biology, University of Edinburgh, Edinburgh, United Kingdom

ARTICLE INFO

Keywords:

PAX6
NEUROG2
Retinoic acid
Neural tube
Transcriptional regulation

ABSTRACT

Proper embryonic development relies on a tight control of spatial and temporal gene expression profiles in a highly regulated manner. One good example is the ON/OFF switching of the transcription factor PAX6 that governs important steps of neurogenesis. In the neural tube PAX6 expression is initiated in neural progenitors through the positive action of retinoic acid signaling and downregulated in neuronal precursors by the bHLH transcription factor NEUROG2. How these two regulatory inputs are integrated at the molecular level to properly fine tune temporal PAX6 expression is not known. In this study we identified and characterized a 940-bp long distal *cis*-regulatory module (CRM), located far away from the PAX6 transcription unit and which conveys positive input from RA signaling pathway and indirect repressive signal(s) from NEUROG2. These opposing regulatory signals are integrated through HOMZ, a 94 bp core region within E940 which is evolutionarily conserved in distant organisms such as the zebrafish. We show that within HOMZ, NEUROG2 and RA exert their opposite temporal activities through a short 60 bp region containing a functional RA-responsive element (RARE). We propose a model in which retinoic acid receptors (RARs) and NEUROG2 repressive target(s) compete on the same DNA motif to fine tune temporal PAX6 expression during the course of spinal neurogenesis.

1. Introduction

During development, formation of the different organs is driven by environmental and intrinsic regulatory signals that fine-tune gene expression both in time and space. This is particularly true during cell fate acquisition, as it often requires rapid and sharp modification of gene expression programs. This genetic control is achieved principally through the action of transcription factors (TFs) that act on genomic *cis* regulatory modules (CRMs), located in nearby non-coding regions or at larger distances from the regulated genes (Spitz and Furlong, 2012). Mutations in these non-coding genomic regions can induce subtle changes in protein levels in specific tissues, leading to developmental defects or diseases (Kleinjan and van Heyningen, 2005). Understanding how positional and temporal cues are interpreted at the genomic level is thus a challenging issue and requires unraveling the functional interactions between transcriptional regulators and CRMs during development.

One important gene for which tight regulation is crucial is the

Paired domain TF PAX6, a master regulatory protein acting as a molecular switch to control cell fate and differentiation in the central nervous system (CNS), olfactory system and pancreas (Cvekl and Callaerts, 2016; Osumi et al., 2008; Simpson and Price, 2002; St-Onge et al., 1997; van Heyningen and Williamson, 2002). It has been shown that PAX6 expression undergoes dosage variation that appears critical for cellular fate. This is evident in the developing eye, in which the loss of one allele of PAX6 gives rise to haploinsufficiency, leading to the eye abnormality aniridia in human and *small eye* in mouse, while the loss of both alleles results in an absence of eyes (Cvekl and Callaerts, 2016). Functional dosage impact has also been observed in the spinal cord where the removal of PAX6 alleles progressively leads to more precocious neuronal differentiation (Bel-Vialar et al., 2007; Sansom et al., 2009). In this tissue, PAX6 is part of a combinatorial TF code that, under the influence of the SHH morphogen, sets up the different progenitor domains, giving rise to the different neuronal subtypes (Ericson et al., 1997; Pituello, 1997). In addition, PAX6 dosage influences important neurogenesis steps. Indeed, while low

* Corresponding author.

levels are permissive for proliferation, increasing PAX6 levels leads to cell cycle exit and neuronal commitment through the activation of the proneural *NEUROG2* gene (Bel-Vialar et al., 2007). Afterwards, PAX6 expression must be extinguished rapidly in committed neuronal precursors in order to allow subsequent neuronal differentiation. PAX6 dosage and temporal regulation therefore controls the timing of neuronal commitment and differentiation. The main molecular players regulating this temporal expression pattern have been identified. Initially, PAX6 expression is maintained OFF in the stem zone of the caudal neural tube through the repressive action of FGF signaling (Bertrand et al., 2000). Then, PAX6 is turned ON in neural progenitors in response to the retinoic acid (RA) signaling pathway (Diez del Corral et al., 2003; Novitsch et al., 2003) and upregulates *NEUROG2*, which in turn represses PAX6 expression in neuronal precursors (Bel-Vialar et al., 2007).

Given the importance of PAX6 temporal regulation for neuronal production, it is important to understand how these different regulatory signals coordinate their action on dedicated PAX6 CRMs to achieve the proper timing of PAX6 expression during neurogenesis. Both RA signaling and *NEUROG2* involve transcriptional regulation. The RA pathway acts through heterodimerization of the retinoic acid receptor (RAR) with the related retinoid X receptor (RXR) that together recognize specific RA Response Elements (RAREs) in the regulatory regions of their target genes (Janesick et al., 2015). *NEUROG2* is a tissue-specific bHLH transcription factor that heterodimerizes with widely-expressed bHLH proteins such as E12 or E47 and classically acts as a transcriptional activator (Bertrand et al., 2002). It can nevertheless inhibit gene expression through three different molecular mechanisms: (1) acting as (or recruiting) a repressor on E-box DNA-binding motifs in the regulatory regions of its target genes (Ross et al., 2003); (2) functioning as a transcriptional activator, upregulating in turn an intermediate transcriptional repressor (Kovach et al., 2013); or (3) acting independently of its ability to bind DNA, via a protein-protein interaction, sequestering the CBP/p300 co-activator (Ge et al., 2006; Sun et al., 2001). Hence, retinoic acid and *NEUROG2* could regulate PAX6 directly or indirectly and could act coordinately or independently through distinct molecular cues. Therefore the identification of PAX6 neural tube CRMs will be an essential step to identify the mechanistic logic behind PAX6 temporal regulation.

Using sequence conservation and DNaseI hyper-sensitivity assays (to identify nucleosome-free chromatin regions), several groups have identified a large number of CRMs within the PAX6 locus, most of them being required for PAX6 expression in the developing eye (Griffin et al., 2002; Kammandel et al., 1999); (Kim and Lauderdale, 2006; Kleinjan et al., 2004; Kleinjan et al., 2006; McBride et al., 2011; Oosterveen et al., 2012; Plaza et al., 1995b; Williams et al., 1998; Xu et al., 1999). Some of these PAX6-specific CRMs are found at a long distance, 3' of the PAX6 encoding sequences, in a large Downstream Regulatory Region (DRR) located within introns of the adjacent ubiquitously-expressed *ELP4* gene, and containing all the aniridia-associated breakpoints identified so far (Griffin et al., 2002; Kleinjan et al., 2004; Kleinjan et al., 2006; McBride et al., 2011). Several DNaseI hyper-sensitive sites have been characterized in the human DRR, named HS1 to HS7, that display tissue-specific expression in the developing eye and telencephalon (Kleinjan et al., 2006; Kleinjan et al., 2001; McBride et al., 2011). However, despite these extensive genomic dissections around the PAX6 locus, the regulatory logic controlling PAX6 expression in the neural tube has not yet been resolved.

In this study, we investigated in more detail the regulatory mechanisms governing the PAX6^{ON/OFF} switching in the developing neural tube. By performing sequence comparison between mammals and birds, chromatin accessibility mapping and functional assays, we identified within the PAX6 locus in the DRR distal region, a new 940 bp CRM (E940) driving specific reporter gene expression in the developing

neural tube and integrating both retinoic acid positive and *NEUROG2* negative signals. Through genomic sequence comparison with evolutionarily more distant organisms and fine functional dissection of E940 (Itasaki et al., 1999), we narrowed down the sequences responsible for positive and repressive activities to a 94 bp core region, called HOMZ, which is also highly conserved in the zebrafish. Using functional tests in the chick, we show that *NEUROG2* induced repression is indirect, involving the activation of an intermediate gene. Finally, we show that *NEUROG2* and RA exert their opposite activity through the same region in HOMZ, which contains a RARE and is enriched in tandemly-repeated predicted binding sites for nuclear receptors. Altogether our data allow us to propose a model in which temporal regulation of PAX6 expression in the neural tube is controlled through a long-range, short DNA enhancer that integrates opposing RA and *NEUROG2* regulatory inputs.

2. Results

2.1. Identification of a neural tube PAX6 CRM driving the retinoic acid and *NEUROG2* response

In order to decipher precisely the logic of Pax6^{ON/OFF} regulation, we needed to identify neural tube-specific PAX6 regulatory regions that could be driven by RA and *NEUROG2* signals. From the literature, two CRMs were described as driving consistent reporter expression in the neural tube in mouse or zebrafish: the mouse GBS (for Gli Binding Site), located within the 7th intron of PAX6 (Fig. 1A), isolated from a screen to find Shh responsive elements, (Oosterveen et al., 2012); and the mouse E55A, located 90 kb upstream of the P1 promoter (Fig. 1A), identified *in silico* by sequence comparison with the elephant shark (Bhatia et al., 2014). The mouse GBS does not contain any putative RAREs but has 2 putative *NEUROG1/2* binding sites, whereas E55A does not contain any predicted RAREs or E-boxes. We nevertheless analyzed these 2 characterized CRMs in light of our objective. E55A is poorly conserved in the chick; it does not drive LACZ expression at an early stage (HH13, Fig. S1) as expected if receiving a RA signal, and it displays only faint activity at a later stage (HH17, Fig. S1). The mouse GBS confers strong GFP expression in the chick neural tube from HH11 to HH17, but it does not respond to either *NEUROG2* or dnRAR overexpression (Fig. S2). We therefore searched for other putative CRMs that could convey PAX6 temporal cues.

To do so, we analyzed the chromatin landscape of the PAX6 locus using ATAC-seq and ChIP-seq data obtained in the mouse embryo at E8.5 and E9.5 (Thierion et al., 2017). We looked at two histone marks associated with enhancers, H3K4me1 and H3K27ac (Zhou et al., 2011) that have been analyzed in mouse whole embryos at E9.5. In parallel, we interrogated in E8.5 and E9.5 mouse embryos, chromatin accessibility in three dissected regions: a part corresponding to rhombomere 3 (r3), rhombomere 5 (r5) and the anterior part of the neural tube, at both (Thierion et al., 2017). As expected, E55A and GBS display high H3K4me1 and H3K27ac enrichment at E9.5 (Fig. S3), consistent with enhancer activity, and we also detected high peaks of accessibility at E55A and GBS positions in neural tube samples (Fig. S3). Interestingly, one of the DNaseI hyper-sensitive sites characterized in the human DRR, HS5 +, located 94 kb downstream of the PAX6 transcription units (Fig. 1A) and showing significant activity in the mouse neural tube in a LacZ reporter assay (McBride et al., 2011), also displays a signature of enhancer chromatin marks (Fig. 1B and Fig. S3). The human HS5 + contains three blocks of high sequence conservation in vertebrates of 940 bp, 83 bp and 821 bp, flanking exon 9 of the *Elp4* gene (Fig. S4). To narrow down the region driving neural tube activity, we examined in more detail the chromatin landscape of this region. In whole embryo extract, HS5 + displays high H3K4me1 enrichment and to a lesser extent some H3K27ac signal (Fig. 1B) suggesting that HS5 + might be active at E9.5. When looking at the chromatin accessibility

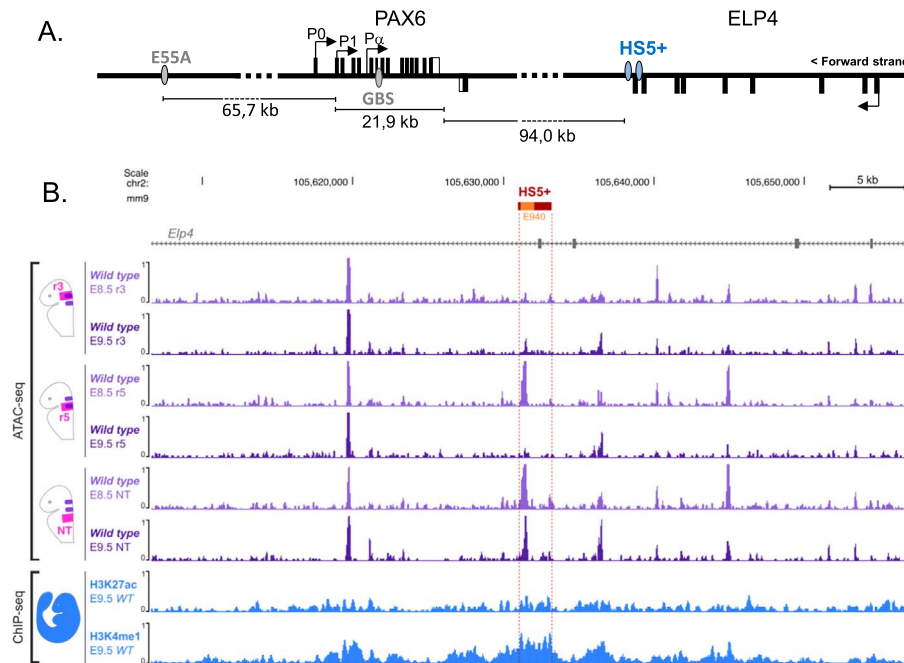


Fig. 1. Identification of a neural tube specific long range *PAX6* CRM. **A.** Schematic representation of the human *PAX6* locus. *E55A*, *GBS* and *HS5 +* positions are indicated. The *HS5 +* region surrounds the exon 9 of the *ELP4* gene, 94 kb downstream of the *PAX6* transcription units. **B.** Chromatin state and accessibility of the mouse *HS5 +*. ATAC-seq was performed on dissected regions (r3, r5 and a more posterior region of the neural tube ("NT") from wild type E8.5 embryos (light purple) and E9.5 embryos (dark purple). ChIP-seq was performed for the H3K27ac and H3K4me1 marks on wild type E9.5 whole embryos (blue). The mouse *Elp4* gene, region *HS5 +* (red), mouse E940 element included in the *HS5 +* (E940, orange) and a genomic scale are indicated at the top.

that has been analyzed specifically in the neural tube and compared to r3 and r5, we detected a high peak at the *HS5 +* position in r5 and neural tube at E8.5, and only in the neural tube at E9.5 (Fig. 1B). This demonstrates local chromatin accessibility at the *HS5 +* genomic region in the neural tube at the time when neurogenesis occurs, confirming the activity of this enhancer in a time and tissue specific manner. Moreover, the peak of open chromatin maps to the most proximal block of *HS5 +* (940 bp). We therefore tested separately the proximal and distal blocks of *HS5 +* in a reporter assay, in the mouse, and found that the 940 bp region was the only one displaying activity in the neural tube (Fig. 2Aa), confirming the result obtained in our chromatin accessibility analysis. We therefore characterized in more detail this small genomic region, from here on called E940.

2.2. E940 recapitulates temporal and spatial cues of *PAX6* expression in the developing neural tube

As observed in Fig. 2Aa, mE940 drives LacZ expression specifically in the neural tube up to the level of r5 and in a narrow region of the brain. We cloned the chick E940 CRM (E940, 911 bp long) and tested its capacity to recapitulate *PAX6* expression, using either a LacZ reporter or a nuclear d2EGFP destabilized reporter to analyze *de novo* the specificity of expression driven by the E940 enhancer. E940 drives significant expression in the chick neural tube as seen with both LacZ and GFP reporters (Fig. 2 and Fig. S5, S6). Co-electroporation of E940d2GFP with a RFP expressing control vector to identify electroporated cells, allowed us to depict precisely the specificity of E940 activity along the antero-posterior and dorso-ventral axes. Consistent activity is detected at early stages (HH11) in the neural tube and caudal hindbrain (Fig. S5). Caudally, E940 drives GFP expression in the transition zone and is not expressed in the stem zone (Fig. S6). This expression profile fits perfectly with normal expression of *PAX6* along the antero-posterior axis at this stage. We then analyzed E940 activity at later stages. At HH15 and HH17, GFP expression is still intense (Fig. S6b-b'''), but it becomes hard to detect in the whole embryo at later

stages (HH18; Fig. S6c-c'''). These observations indicate that similar to endogenous *PAX6* expression, E940 driven GFP signal is progressively narrowed down dorso-ventrally to the medial part of the ventricular zone during the course of neural tube maturation. In agreement with the mouse ATAC-seq data, E940 confers expression in r5 at stage HH11 but not HH17, corresponding to E8.5 and E9.5 in the mouse, and is never active in r3 (Fig. S5). When examined carefully in the D-V axis at HH15, only a subset of electroporated cells expresses the GFP, all located in the *PAX6* expression domain (Fig. 2B). The GFP is now restricted to few cells in the medial region of the ventricular zone (Fig. 2C), consistent with the faint GFP signal observed in the whole embryo at this stage (Fig. S6c-c'''). Immunostaining of NEUROG2 shows that some GFP positive nuclei co-express low or intermediate levels of NEUROG2, consistent with our previous study showing that NEUROG2 is progressively upregulated in *PAX6* positive cells, up to a critical threshold required to downregulate *Pax6* via a feedback mechanism (see Fig. 8 in (Bel-Vialar et al., 2007)). However, as expected from this same study, and consistent with the non-expression of *PAX6* in neurons, we couldn't detect any GFP signal in electroporated cells expressing the neuronal marker HuC/D, (Bel-Vialar et al., 2007).

In order to test whether E940 contains the molecular cues necessary to control *PAX6*^{ON/OFF}, we electroporated the E940d2GFP reporter together with either a dominant negative form of the RAR alpha (dnRAR), to block the RA pathway, or with NEUROG2. The overexpression of dnRAR or NEUROG2 completely abolished the expression of E940d2GFP compared to a control vector (Fig. 2D). To quantify this effect we used a dual luciferase assay, with a construct in which E940 drives the expression of firefly luciferase (E940Luc). We observed that blockade of the RA pathway or NEUROG2 overexpression leads to a strong decrease in E940Luc expression (Fig. 2D) (140 and 30 fold change respectively). This data indicates that E940 conveys both retinoic acid positive activity and NEUROG2 repressive activity.

Altogether, these data show that this long range CRM integrates temporal cues for *PAX6* regulation in the neural tube.

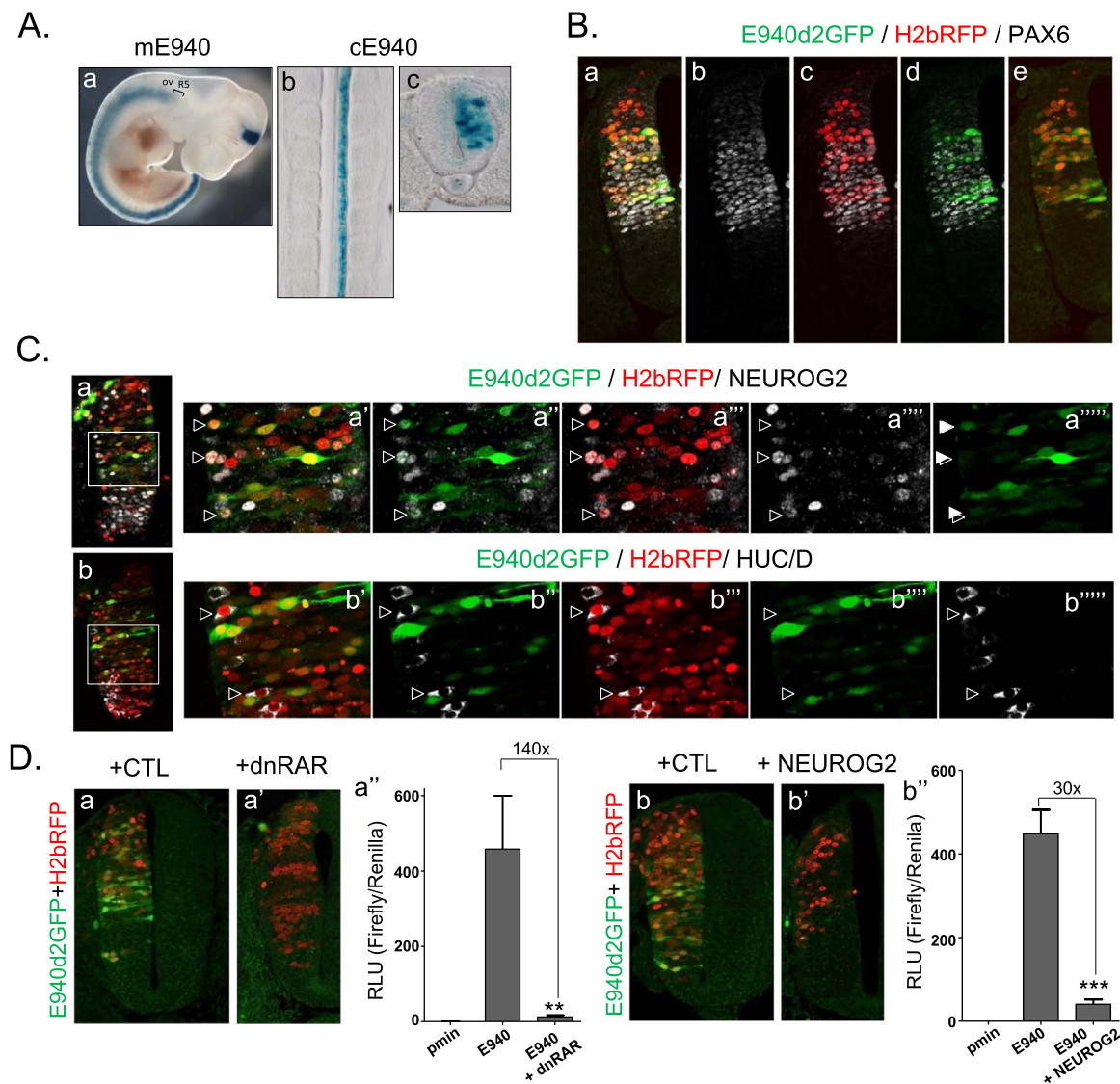


Fig. 2. E940 recapitulates temporal PAX6 expression during neurogenesis. **A.** Expression of a *LACZ* reporter gene under the control of the mouse E940 in a 10.5 dpc embryo from a transgenic line (a) or the chicken E940 (cE940) in a stage 15 electroporated chick neural tube (b, c). **B.** Expression of a d2GFP destabilized under the control of cE940 in a transversal section of electroporated neural tube (a–e). In red is the RFP signal given by a control vector co-electroporated with pLAC00E940-GFP. The GFP signal overlaps with the endogenous PAX6 protein detected in far red by immunohistochemistry. **C.** Stage HH17 chick embryos electroporated at HH12 with cE940d2GFP + H2bRFP. The GFP signal progressively decreases in NEUROG2 positive cells (arrowheads NEUROG2^{low}, GFP^{low} cells) and is completely extinguished in neurons labeled with HUC/D (arrowheads). **D.** Electroporation of dnRAR (a, a') or NEUROG2 (b, b') abolishes the activity of cE940 (GFP in green). In red the RFP signal is given by a control vector electroporated at the same time. (a'') and (b'') are histograms showing the relative luciferase signal (RLU) of the luciferase firefly under the control of a minimal promoter (pmin, n = 4 in a''; n = 9 in b'') or E940 (pmin-E940, n = 5 in a''; n = 9 in b'') co-electroporated with a control vector, dnRAR (n = 5) or NEUROG2 (n = 9). P value < 0.001 ***, P value < 0.01 **, Mann-Whitney test.

2.3. Three E940 subregions are sufficient to recapitulate the whole CRM activity

In order to identify which subregions are important for E940 activity, we performed a functional dissection using a dual firefly and Renilla luciferase assay (Fig. 3A). We first tested a series of fragments lacking either the 3' part (E940A), the 5' part (E940B) or deleted from both ends (E940C). Only E940B and E940C display noticeable activity, indicating that a region located in E940B and E940C but absent in E940A is critically required (Fig. 3A). By analyzing sequence conservation among species (Fig. S7), we found that E940B and E940C contain all or part of a 94 bp length region in E940 that shows strong conservation in zebrafish and that we called HOMZ for HOMologous to Zebrafish (Fig. S7 and Fig. 3B). Moreover, the peak observed in the ATAC-seq data is centered in this HOMZ region in the neural tube (Fig. 3C). We therefore analyzed the

importance of this evolutionarily-conserved region by testing an E940 version specifically deleted for HOMZ (E940delHOMZ). This deletion leads to a strong decrease in E940 activity, indicating that the HOMZ region conveys a strong positive activity (Fig. 3A). However when tested on its own, HOMZ did not drive any activity, indicating that HOMZ is the core region of E940 and needs to be combined with other E940 parts to recapitulate full E940 activity. As E940C, which contains HOMZ, is not sufficient for full activity, we hypothesized that regions on the 5' and/or 3' ends absent from E940C must also be required for the robustness of expression. We tested a series of deletion constructs keeping the HOMZ core region intact and identified that a construct linking the 5'-most and 3'-most sub regions to HOMZ (5'+HOMZ+3'), 412 bp long, recapitulates the complete E940 activity (Fig. 3A). We thus identified three sub-regions, 5'-E940, HOMZ and 3'-E940, that synergize to drive high reporter expression specifically in the neural tube.

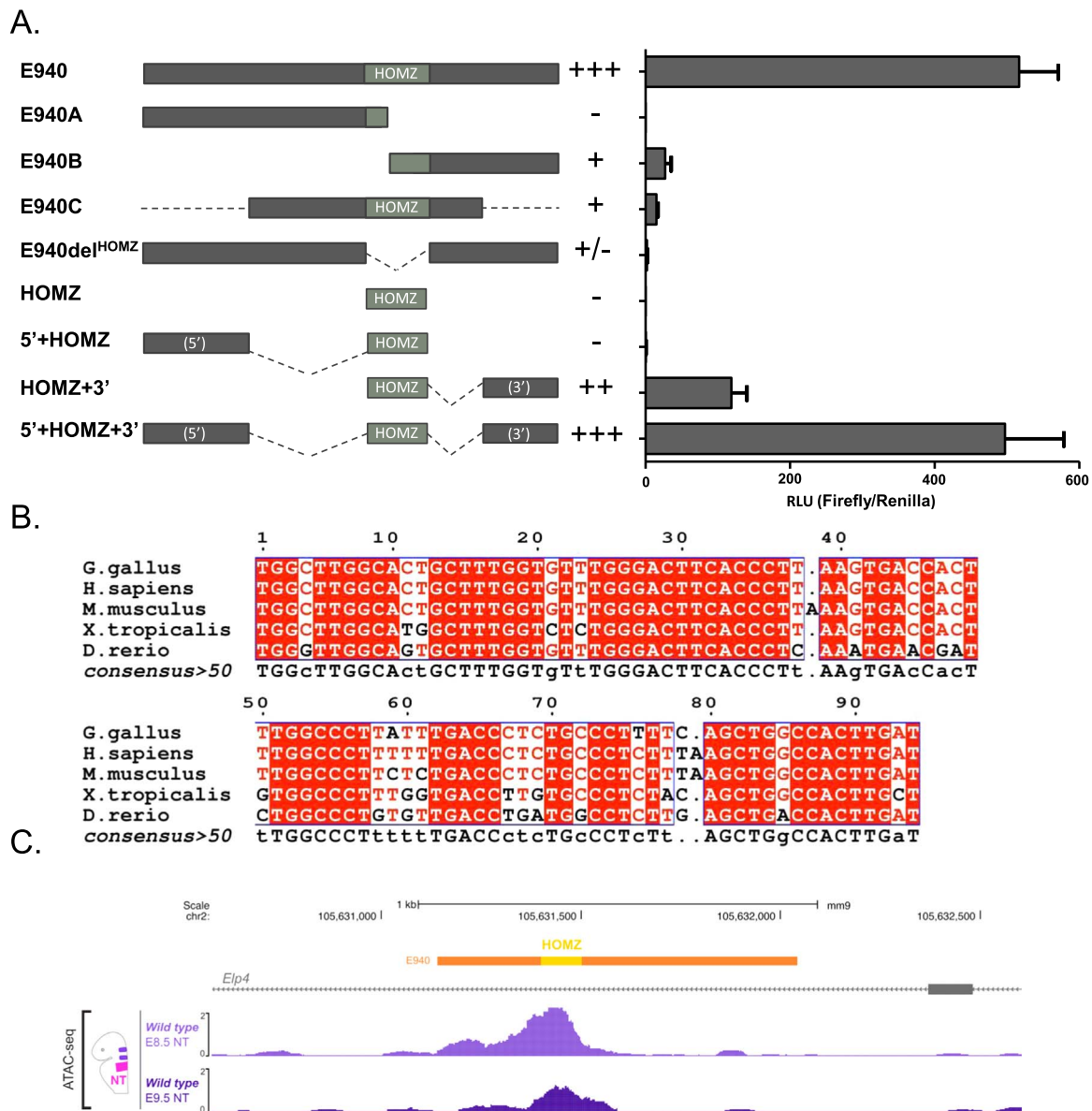


Fig. 3. Three sub-regions of the E940 CRM synergize for full activity. **A.** Graphical representation of the enhancer regions tested for their luciferase activity in and corresponding RLU measures ($n = 3$ to 23). **B.** HOMZ conservation among vertebrates (from 529 to 623 bp in the chick E940 sequence). Strictly conserved residues are in white on a red background, whereas partially conserved ones are depicted in red on a white background. A consensus sequence is shown in beneath with strictly or partially conserved residues in upper or lower case characters, respectively. **C.** Chromatin state and accessibility of the mouse region HOMZ. ATAC-seq was performed on dissected neural tube ("NT") from wild type E8.5 embryos (light purple) and E9.5 embryos (dark purple). The mouse E940 element (orange), HOMZ (yellow) and a genomic scale are indicated at the top.

2.4. Retinoic acid controls E940-driven neural tube expression through three scattered RARE sites

Given that E940 activity responds to retinoic signaling, we wondered which part of E940 is involved in this response. We searched *in silico*, using the genomatrix software, for putative RARE elements in the entire E940 (Cartharius et al., 2005). RAR-RXR heterodimers preferentially bind response elements comprised of two AGGTCA sites arranged as direct repeats, with specific inter-half-site spacings of 1–5 bp (known as DR1–DR5, respectively; (Umesono et al., 1991; Mangelsdorf and Evans, 1995)). We found three putative DR1 or DR5 binding sites, two located in the 5'-E940 region (DR1) and one in HOMZ (DR5) (Fig. 4A, matrix similarity of 0.786, 0.812 and 0.858, respectively). To determine the importance of these RAREs for E940 positive activity, we mutated them separately or together within E940 (Fig. 4A) and compared their activity using GFP or luciferase reporter

assays (Fig. 4B, C). Single base pair mutations in any of the 3 RAREs or in all of them together, lead to a strong reduction in E940 activity (Fig. 4B, C). Interestingly, mutation in the RARE3 alone has the same effect as mutating all three RAREs together, suggesting that it has preponderant importance when compared to RARE 1 and RARE2. We then asked whether E940 and HOMZ were responsive to retinoic acid positive input. We electroporated E940Luc, E940mutRAR123Luc or HOMZLuc with RAR-VP16, which is a constitutively active form of the RAR alpha receptor (Blumberg et al., 1997). Both E940 and HOMZ respond to RAR-VP16 (Fig. 4D, E). In addition, we tested if HOMZ activity was responsive to dnRAR. As it doesn't drive any detectable activity we combined it with a well-characterized minimal enhancer, showing weak activity in the neural tube (E^{\min} , (Moore et al., 2013), see methods), that should allow us to bypass the detection threshold. E^{\min} HOMZ drove positive activity (Fig. S9) and as expected, it is negatively responsive to dnRAR (Fig. 4E). We then tested if mutation of the 3

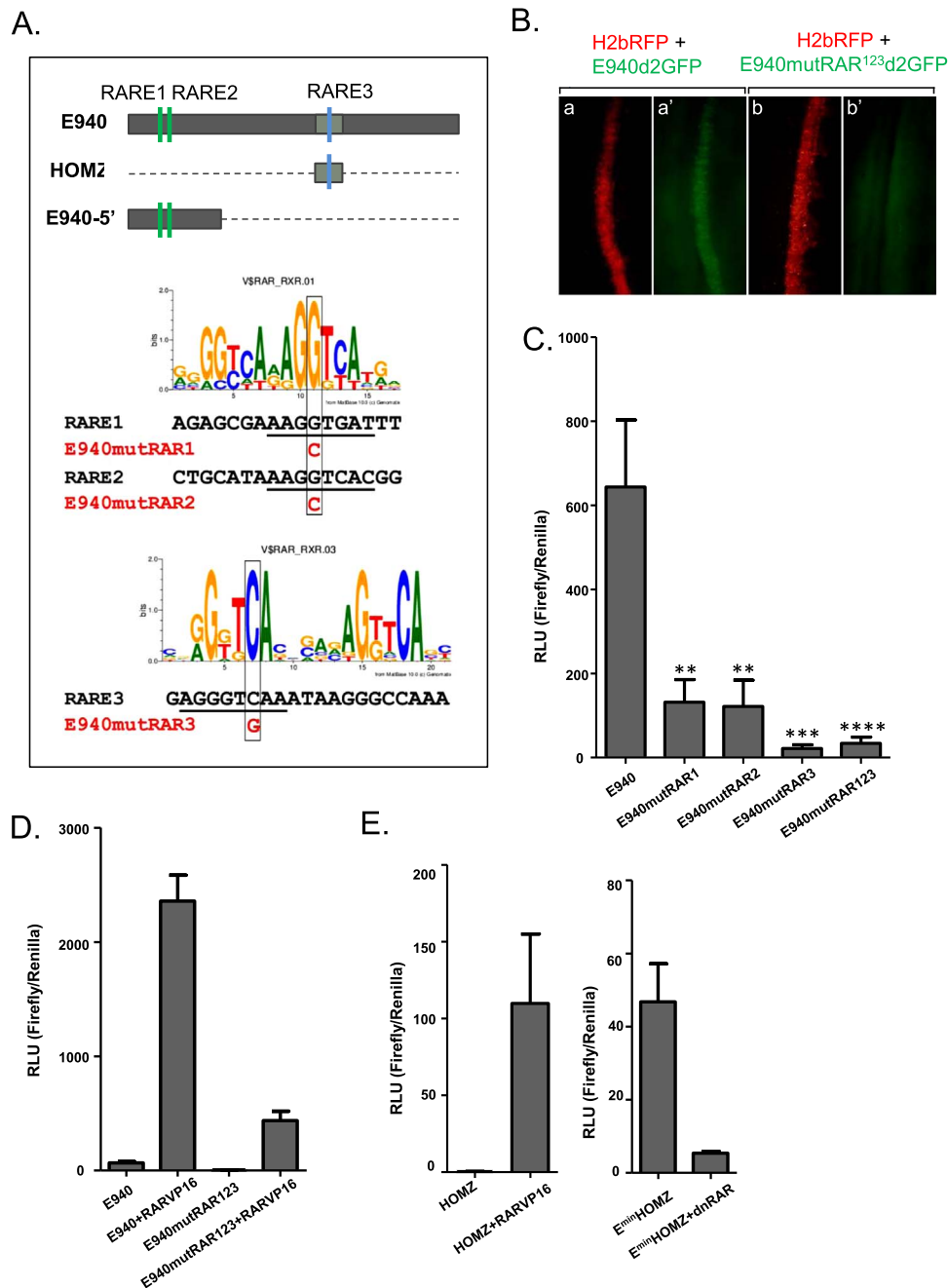


Fig. 4. Three RAREs collaborate on E940 to drive retinoic acid response. **A. On top:** Graphical representation of the position of the RAREs (green and blue bars) in E940 (dark grey) and HOMZ (light grey). **Bottom:** Alignment of RARE1 and RARE2 with the RAR/RXR heterodimer DR1 site (random expectation of 0.07 matches per 1000 bp) and alignment of RARE3 with the RAR/RXR heterodimer DR5 site (random expectation of less than 0.01 matches per 1000 bp), from MatBase 10.0, Genomatix. In red, the one bp replacements that were performed in each of the 3 RAREs to generate mutated versions of cE940: E940mutRAR1, E940mutRAR2, E940mutRAR3. The E940mutRAR123 contains all three mutations. **B.** Dorsal view of neural tubes electroporated with pLAC00E940-GFP (a, a') or pLAC00E940mutRAR123-GFP (b, b') constructs and a pRFP control vector. Note that simultaneous mutation of the 3 RAREs strongly diminishes E940 activity (b, b'). **C.** Quantitative measure of the activity of the E940 mutated forms in luciferase assays. (E940, n = 10; E940mutRAR1, n = 10; E940mutRAR2, n = 7; E940mutRAR3, n = 11; E940mutRAR123, n = 8). All the mutated forms display a strong reduction of activity if compared to native E940; P value < 0.0001 ****, P value < 0.001 ***, P value < 0.01 **, Mann-Whitney test. **D.** Comparison of the effect of RAR-VP16 on E940 and E940mutRAR123 in luciferase assays (E940, n = 3; E940mutRAR123, n = 3). **E.** Quantitative measure of the response of the core enhancer HOMZ to RA signaling (HOMZ, n = 3; HOMZ+RAR-VP16, n = 3; E^{min}HOMZ, n = 3; E^{min}HOMZ+dnRAR, n = 3).

RAREs was sufficient to abolish RA activity and indeed, E940mutRAR123 is less sensitive to RAR-VP16 than E940 (Fig. 4D), confirming the importance of RAREs 1–3 for driving RA positive input. These data argue that the three predicted RAREs recapitulate most of their activity and act synergistically to transduce an RA positive regulatory signal.

2.5. The regulatory link between *NEUROG2* and *PAX6* is conserved in the zebrafish

As HOMZ is also present in the zebrafish genome, we performed additional experiments in the fish to determine if the regulatory link between *NEUROG2* and *PAX6* that we described in the chick has been

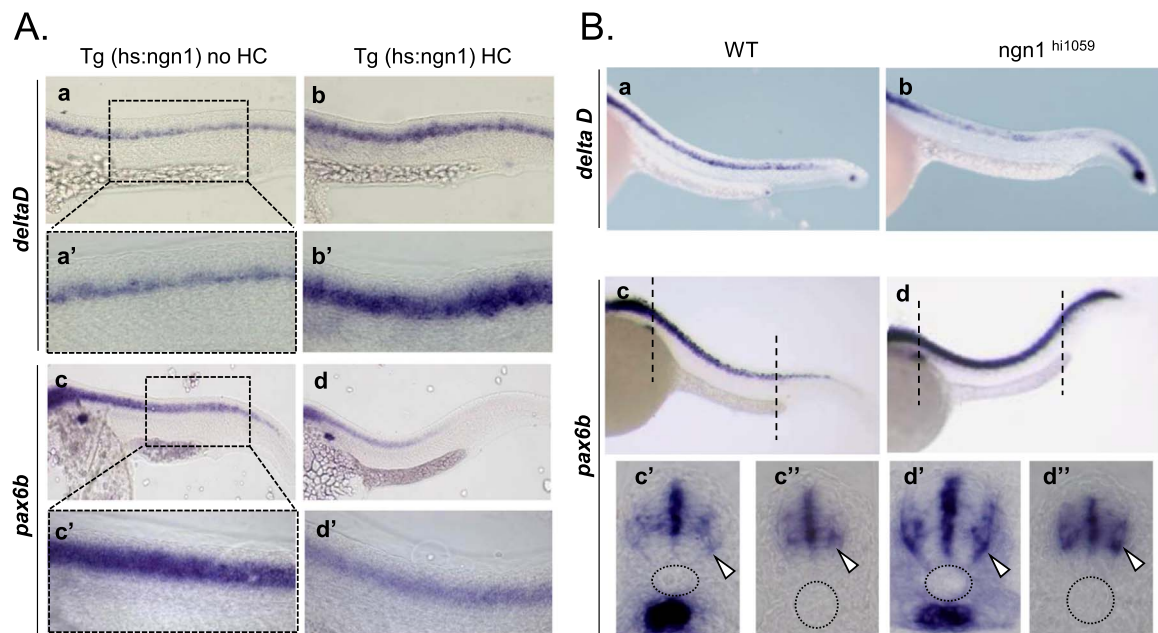


Fig. 5. The NEUROG2/PAX6 regulatory link is conserved in the zebrafish. **A.** Expression of *deltaD* and *pax6b* in zebrafish embryos expressing the *ngn1* transgene under the control of a *hsp70* heat shock (HS) inducible promoter. *deltaD* expression in non-heat shock (a, a', n = 10) and heat shock *ngn1* transgenic embryos (b, b', n = 5). *pax6b* expression in non-heat shock (c, c', n = 15) and heat shock *ngn1* transgenic embryos (d, d', n = 5). *deltaD* is induced and *pax6b* is repressed when *ngn1* is overexpressed upon HC (compare b'to a' and d' to c' respectively). **B.** Expression of *deltaD* and *pax6b* in zebrafish embryos invalidated for *ngn1* (*ngn1*^{hi1059}) and WT embryos. *deltaD* expression is downregulated in the absence of *ngn1* function (compare a (n = 20) and b (n = 10)). *pax6b* is upregulated in *ngn1*^{hi1059} (compare c (n = 30) to d (n = 15)). Transversal section of WT or *ngn1*^{hi1059} embryos showing that *pax6b* expression is maintained at the border of the neural tube where neuronal precursors are located (compare d, d' to c, c', c''). Dashed circle mark the position of the notochord.

conserved throughout evolution. In the zebrafish, the NEUROG1/2 closest homolog is *neurog1* (Blader et al., 1997), and PAX6 has been duplicated in two paralogous genes, *pax6a* and *pax6b* (Kleinjan et al., 2008; Ma et al., 1996; Nornes et al., 1998). In the neural tube, *pax6b* expression is stronger than *pax6a* (data not shown), we thus decided to focus on *pax6b* expression. We also analyzed the expression of *deltaD*, the zebrafish homolog of Delta that is a well-known proneural positive target gene (Chitnis et al., 1995; Ma et al., 1998). We first analyzed their expression in a heat-shock inducible *neurog1* transgenic line (Fig. 5A). As expected for a positive NEUROG1/2 target, *deltaD* expression is strongly activated upon heat shock (Fig. 5A a-a' and b-b'). In contrast, *pax6b* expression is downregulated in the heat shock condition (Fig. 5A c-c', d-d'). This result indicates that *neurog1* represses *pax6b* expression in the zebrafish neural tube, similar to the situation seen in the chick embryo.

We further took advantage of this genetic model to determine if neurogenin activity is necessary for *pax6b* repression, using a zebrafish mutant line in which *neurog1* expression is strongly impaired (Golling et al., 2002). As anticipated, *deltaD* is firmly downregulated in this mutant (Fig. 5B a, b), and *pax6b* expression is specifically upregulated in neuronal precursors where *neurog1* would normally be present (Fig. 5B d-d'). These results show that the NEUROG1/2/PAX6 regulatory loop has been conserved during vertebrate evolution. In addition, they reinforce our previous data by showing that NEUROG1/2 is necessary to extinguish PAX6 expression in neuronal precursors.

2.6. Repression by NEUROG2 is indirect and requires an intermediate gene

We next investigated the molecular mechanism by which NEUROG2 represses PAX6 expression. As mentioned in the introduction, NEUROG2 can repress its target genes by different mechanisms. To distinguish between the various possibilities, we tested the capability of different mutant forms of NEUROG2 to repress PAX6 expression in chick neural tube. We performed an *in silico* search for neurogenin specific E-boxes and did not find any predicted sites in

E940 (not shown). In a previous study, we showed that DNA-binding to E-boxes is necessary for this repression, by electroporating NEUROG2-AQ, a mutant form containing a two amino-acid substitution in the C terminus of the basic domain that abolishes binding to E-boxes and leads to loss of neurogenic activity (Fig. 6A b-b' and (Lacomme et al., 2012)). Here we asked whether protein-protein interaction with the CBP/p300 co-activator is also involved in this repression, using NEUROG2-YA, in which tyrosine Y241 is converted to alanine, which abolishes the interaction with CBP/P300 without affecting neurogenic activity (Ge et al., 2006; Lacomme et al., 2012; Sun et al., 2001). We electroporated NEUROG2-YA in the neural tube of HH11 chick embryos and found that it drives strong PAX6 inhibition after 6 h, similar to the effect of overexpressing a native form of NEUROG2 (Fig. 6A c-c' and a-a'), indicating that PAX6 repression only requires binding to E-boxes and is not due to CBP/p300 sequestration.

In order to determine whether the repression is direct or indirect, we next compared the repressive potential of NEUROG2-ENR, a constitutive repressor form of NEUROG2, or NEUROG2-VP16, a constitutively active form (Dixit et al., 2014) on PAX6 expression. Electroporation of NEUROG2-VP16 mimicked the effect of the native NEUROG2 gain-of-function, whereas NEUROG2-ENR had no effect (Fig. 6A, d-d' and e-e' and (Lacomme et al., 2012)). Altogether these experiments indicate that NEUROG2 activates one or several repressor gene(s) that in turn inhibit(s) PAX6 transcription.

2.7. NEUROG2 driven repression relies on the HOMZ core region

The next step was to determine which E940 sub-region(s) mediate(s) NEUROG2 driven repressive activity. To do so we co-electroporated different E940 sub-regions with or without NEUROG2 and performed the previously-used dual luciferase assay. The activity of E940, 5'+HOMZ+3' and E940C was strongly repressed by NEUROG2 (Fig. 6B and Fig. S8), suggesting that HOMZ, which is the only shared fragment between these three constructs, might be the region driving NEUROG2 negative activity. The HOMZ+3' combination also displays a consistent NEUROG2 response, while the 5'+HOMZ construct could

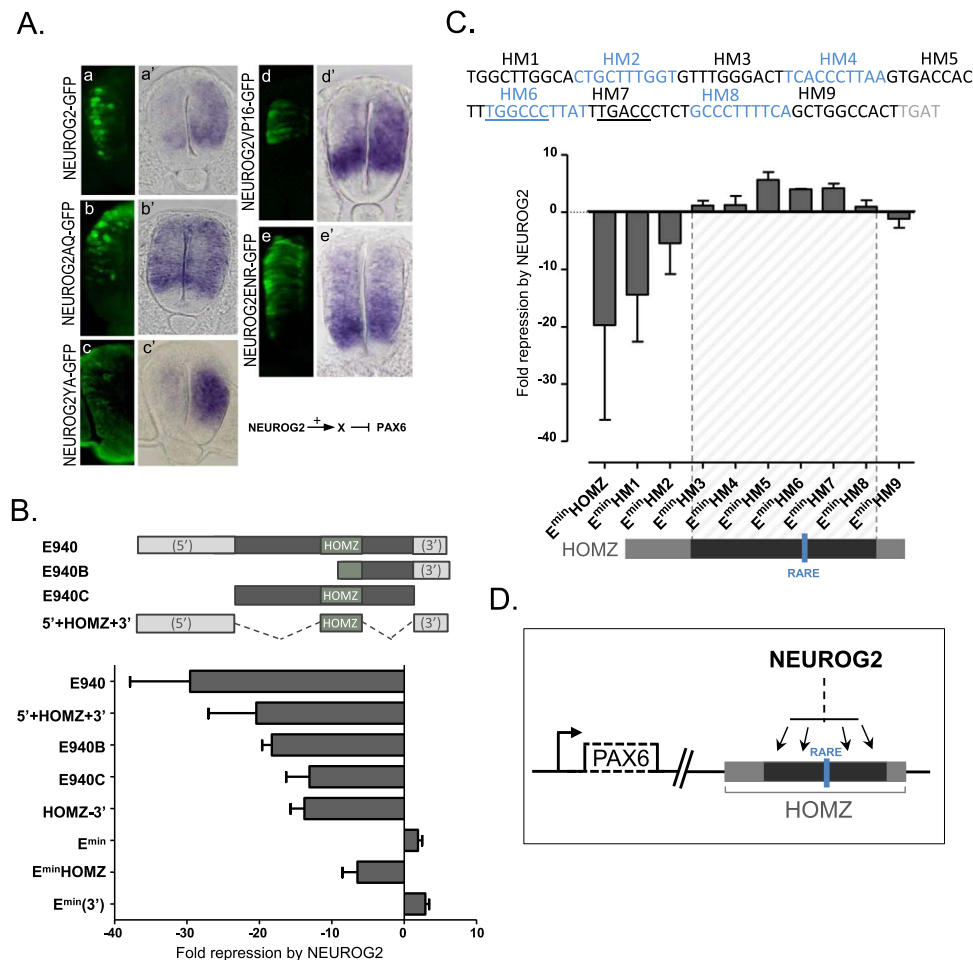


Fig. 6. NEUROG2 acts indirectly through a 60bp region in HOMZ. **A.** In situ detection of chicken PAX6 mRNA on HH12 chicken neural tube sections electroporated with the mentioned constructs (co-expressing the GFP, in green). **B.** Comparison of the repressive effect of NEUROG2 on the activity of different regions of the E940 enhancer in luciferase assays. Only HOMZ activity is repressed by NEUROG2. **C. On top:** Graphic representation of the 10 by 10 bp replacement (HM mutations) performed on the HOMZ element fused to E^{min} (see methods). Underlined are the two half sites of the RAR-RXR RARE3 binding motif. **On bottom:** comparison of the effect of NEUROG2 on the activity of the different E^{min} HM forms in luciferase reporter assays. The light gray bar schematizes HOMZ with a dark gray zone corresponding to the 60 bp region necessary for NEUROG2 repression. **D. Model:** Repression of PAX6 transcripts by NEUROG2 in the neural tube involves the activation of an intermediate repressor protein and requires a 60 bp sequence on HOMZ that also contains RARE3.

not be tested due to its absence of activity. In addition, E940B, containing only part of HOMZ, responds to NEUROG2, suggesting that the repressive activity is contained in the 3' part of HOMZ (Fig. 6B and Fig. S8). Due to the faint expression driven by 5'-E940, HOMZ and 3'-E940 alone (Fig. 3A and not shown), we could not directly test if their drive NEUROG2 repressive activity. We therefore tested for repression on combined forms linking 5'-E940, HOMZ or 3'-E940 regions with the minimal enhancer E^{min} (Moore et al., 2013). When combined with E^{min} , the 5'-E940 region combination (E^{min} (5')) led to reduced activity when compared to E^{min} alone, whereas HOMZ (E^{min} HOMZ) and 3'-E940 (E^{min} (3')) drove positive activity (Fig. S9). It was still not possible to test 5'-E940, owing to its inability to drive any positive activity on its own or combined with E^{min} . However, we tested repression by NEUROG2 of HOMZ and 3'-E940 using the E^{min} -fused versions. Having verified that E^{min} alone does not respond to NEUROG2 signaling (Fig. 6B and Fig. S10), we observed that E^{min} HOMZ is repressed by NEUROG2, whereas E^{min} (3') is insensitive or even slightly activated by NEUROG2 (Fig. 6B and Fig. S8). These data thus indicate that in addition to RA driven positive activity, the HOMZ core region is also required for NEUROG2-mediated repressive activity.

The fact that E940B, which lacks the first 39 bases of HOMZ (E940B sequence ranges from 568 to 911 bp of E940, Fig. S7), is

completely repressed by NEUROG2, allowed us to narrow down the DNA sequence required for repression to between 40–94 bp of the HOMZ CRM. Interestingly, this region also contains the DR5 RAR-RXR DNA binding site (RARE3) that we identified as necessary for the RA signaling response. In order to identify which DNA motif inside this 40 to 94 bp region is required for NEUROG2 driven repression, we performed a “linker scanning” experiment by replacing every 10 bp of E^{min} HOMZ with a scrambled DNA sequence. We thus generated 9 modified HOMZ versions (HM1 to HM9) and tested each one in the dual luciferase assay for their expression and response to repressive NEUROG2 (see methods, Fig. 6C and Fig. S11). This approach confirmed that the region between base 40 and base 94 is important for HOMZ positive activity (Fig. S11). Even though some HM forms only maintained faint activity (HM5 to HM7, Fig. S11), we nevertheless tested all of them for repression by NEUROG2. We found that replacement of any 10 bp portion between the 30th (HM3) and the 80th (HM8) base pair of the HOMZ sequence impeded repression by NEUROG2 (Fig. 6C and Fig. S12). The least active forms, HM5, HM6 and HM7, even became slightly activated, likely due to the presence of the E^{min} enhancer. This functional dissection of the HOMZ core enhancer indicates that NEUROG2 repressive activity is not restricted to a single DNA binding motif but channeled through a 60 bp long region inside HOMZ, also containing the RARE3 binding site (Fig. 6D).

2.8. Repressive *NEUROG2* and activating *RA* signals act through the same DNA motif

As repressive and activating signals are acting through the same 60 bp DNA region, it raises the possibility that *RA* and *NEUROG2* driven signals share the same DNA motif and compete to fine tune the ON/OFF of *PAX6* expression. It has been described that *NEUROG2* can physically interact with *RAR* receptors, tethering them to E-box sites and controlling gene expression in motoneurons (Lee et al., 2009). In view of this data, the possibility existed that the reduction of E940 activity upon *NEUROG2* overexpression was due to unspecific sequestration of *RARs* away from their own DNA binding sites. If it were the case, *NEUROG2AQ* should have the same effect as *NEUROG2* on the activity of E940, as it retains the capacity for protein-protein interaction while being unable to bind to E-boxes. We show that this is not the case, as *NEUROG2AQ* is highly inefficient at repressing E940-Luc (Fig. S13). However, downregulation of E940 activity could still be due to an indirect sequestration of *RARs* by the *NEUROG2* target. We reasoned that if the effect of *NEUROG2* was due to *RARs* sequestration, E940mutRAR123 activity shouldn't be modulated by *NEUROG2*. Alternatively its activity should be downregulated as efficiently as for the E940 WT form. To test this we co-electroporated *NEUROG2* with either the wild-type E940 or E940mutRAR123 reporter construct and quantified the activity of these two CRMs in the dual luciferase assay. As shown in Fig. 7A, the expression driven by E940mutRAR123 is still repressed efficiently by *NEUROG2*, indicating that repression by *NEUROG2* is not an indirect effect due to sequestration of *RARs* receptors away from the RARE sites. Moreover, *NEUROG2* repressive activity on E940mutRAR123 was even stronger than on the native E940 form (Fig. 7A), suggesting that mutation of RAREs tips the regulatory balance in favor of repression by *NEUROG2*. As we have shown that *NEUROG2* acts through the HOMZ core region, this suggests that it is the mutation in RARE3 that favors repression by *NEUROG2*. We therefore compared the repression of E940mutRAR1 to that of E940mutRAR3, reasoning that E940mutRAR1 should not be more repressed than wildtype E940 as RARE1 is located outside the HOMZ region, whereas E940mutRAR3 should be as sensitive as the E940mutRAR123 construct to repressive *NEUROG2* activity. Indeed we found that E940mutRAR3 is subject to repression by *NEUROG2* at the same level as E940mutRAR123, and that E940mutRAR1 is repressed to the same level as native E940 (Fig. 7 A, B). Thus, repression downstream of *NEUROG2* seems a more favored response specifically when the RARE3 site is mutated, suggesting that *RAR-RXR* heterodimers and *NEUROG2* induced-repressor(s) physically compete through the same DNA motif within HOMZ to finely regulate *PAX6*^{ON/OFF} status.

To clarify this issue, we performed competition experiments using a mutated form of *RAR*, *RAR*^{delAF2}, which is able to bind to RAREs but lacks part of its heterodimerization domain and does not interact with co-activators such as CBP/p300 (Lee et al., 2009). We hypothesized that *RAR*^{delAF2} would sterically block the RAREs on E940 without significantly modifying the *RA* response, as *RAR* mutants lacking both the delta AF2 domain and the dimerization domain have been reported to have negligible dominant negative activity when compared to dn*RAR*, which retains the dimerization domain (Blumberg et al., 1997; Lee et al., 2009). As seen in Fig. 7C, *RAR*^{delAF2} indeed fails to perturb E940 activity (Fig. 7C c, c'). However when co-electroporated with *NEUROG2*, it blocks the ability of *NEUROG2* to inhibit E940 driven GFP signal (Fig. 7C d, d'). We quantified the effect of *NEUROG2* and *RAR*^{delAF2}, alone or in combination, in our luciferase assay and confirmed that *RAR*^{delAF2} does not alter E940 activity but strongly impedes the repressive activity of *NEUROG2* on E940 (Fig. 7D; ~80 FC repression with *NEUROG2* and ~2 FC with *NEUROG2*+ *RAR*^{delAF2}). These experiments indicate that *RARs* compete with *NEUROG2* on HOMZ to control E940 activity.

The observation that any 10 bp replacement between bp 40 to 90 on

the HOMZ region impedes *NEUROG2* repression, suggests that several TFs act together or synergistically to repress *PAX6* expression, or that clustering of binding sites for the same transcriptional repressor is needed, and that these TFs bind within a 60 bp region surrounding the HOMZ RARE (RARE3). We therefore searched for putative TF binding sites in the vicinity of the RARE. *In silico* analysis revealed a significant enrichment of binding sites for potent genes in the nuclear receptor (NR) superfamily (Fig. 7E). Significantly, the binding sites are remarkably regularly spaced and similarly oriented. All the linker scanning replacements affecting *NEUROG2*-dependent repression (HM4 to HM8) affect at least one of these predicted sites (compare Figs. 7E and 6B), suggesting that a subset of nuclear receptors could act cooperatively to repress *Pax6* expression downstream of *NEUROG2*.

All together our results suggest a model in which *RA* and the *NEUROG2* target gene(s), which could be members of the NR superfamily, share DNA motifs in close proximity on E940 to control *PAX6* temporal expression during the course of spinal neurogenesis (Fig. 7F). Further investigation will be necessary to decipher if orphan nuclear receptors or some of their co-factors are involved in this balanced temporal regulation.

3. Discussion

In this study we have characterized a new CRM, E940, which controls the temporal dynamics of *PAX6* expression in the chicken neural tube. This highly conserved CRM is located at quite a long distance downstream of the *PAX6* gene and responds to *RA* driven positive and *NEUROG2* driven negative signals. We show that within E940, these regulatory signals switch *PAX6* on or off in the developing neural tube through a 94 bp core region, HOMZ, which is highly conserved in the zebrafish. Moreover, we identified 3 RAREs that trigger most of the positive retinoic acid response and showed that the repression by *NEUROG2* involves the activation of one or several intermediate factor(s). In addition we showed that *RA* and *NEUROG2* regulatory signals compete through a 60 bp DNA region in HOMZ to exert their opposing effects on *PAX6* expression. Altogether, our results present an important step forward in identifying the spatio-temporal regulatory logic of *PAX6* expression in the developing neural tube. The high density of predicted nuclear receptor binding sites within HOMZ suggests a scenario that could also implicate this gene family in the temporal ON/OFF switching of *PAX6* expression.

3.1. E940: A temporal control element

It is now well established that gene expression is often controlled not just by one but by several CRMs that collaborate to reinforce robustness of expression patterns and that allow a more delicately fine-tuned temporal and spatial regulation (Spitz and Furlong, 2012). This is particularly true for *PAX6* regulation, as the transgenic reporter studies that have been performed so far have identified a large number of CRMs with overlapping tissue specificities. Collectively these data suggest that for various tissues, several CRMs cooperate within the endogenous locus. Here we show that E940 controls the temporal aspect of *PAX6* expression in the developing neural tube. E940 activity starts at the level of the transition zone, caudally, where retinoic acid signaling starts to be active (Diez del Corral et al., 2003) and spans the entire A-P axis of the neural tube. In addition, in agreement with the dynamics of endogenous *PAX6* expression during the different steps of neurogenesis (Bel-Vialar et al., 2007), E940 is active in neural progenitors but is progressively silenced in differentiating neuronal precursors, as seen when compared to *NEUROG2* and *HuCD* expression. Consistent with ATAC-seq data obtained in the mouse, E940 drives GFP expression in r5 at early embryonic stages but is never active in r3. However, it has been shown that *PAX6* is expressed in r3/r5 from HH10 to at least HH17 (Kayam et al., 2013). E940 therefore does not contain regulatory cues for *PAX6* expression in the hindbrain,

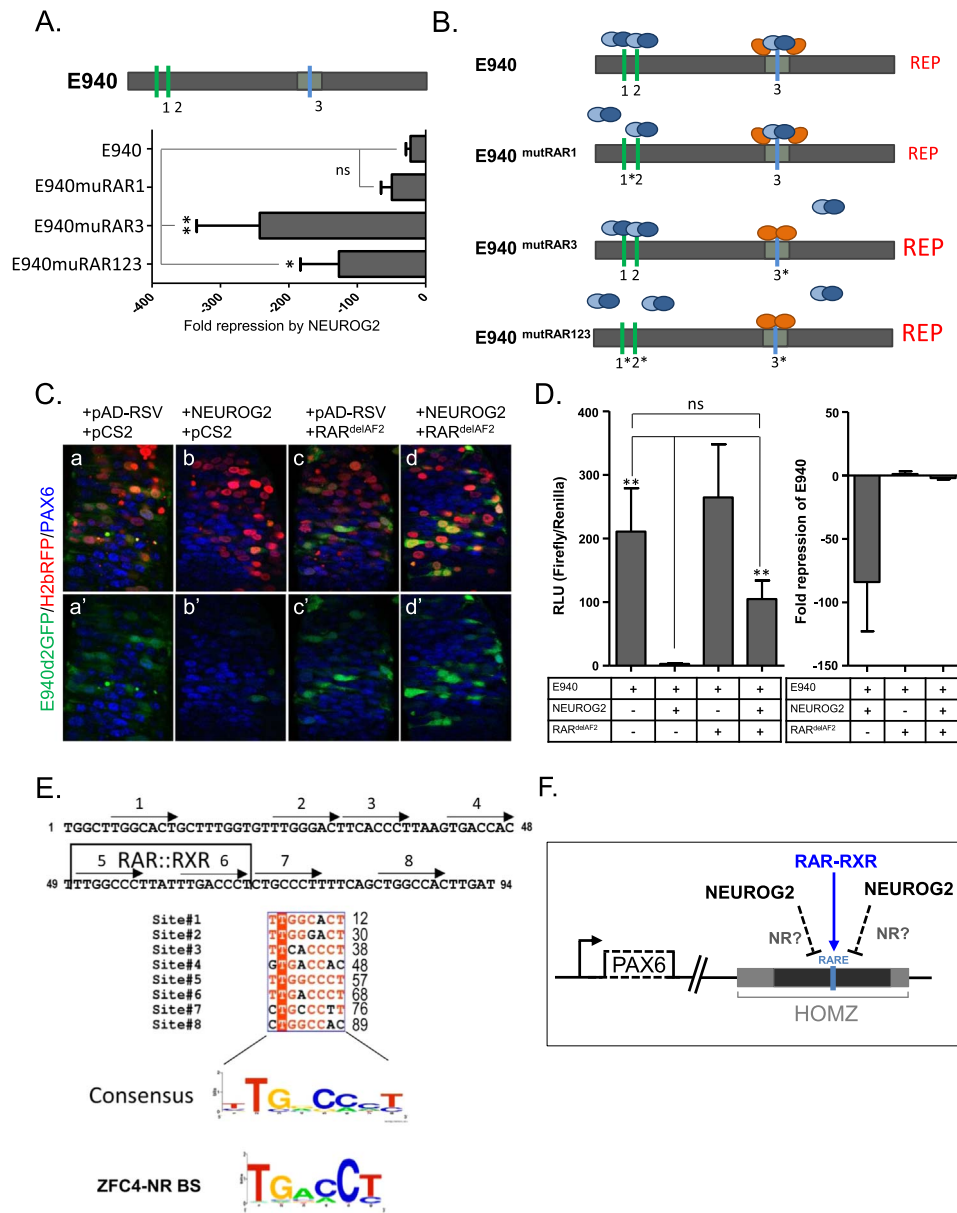


Fig. 7. NEUROG2 and RA exert their opposite activities through competition on a 60 bp region enriched in NRs putative DBS on HOMZ. **A.** Comparison of the repressive effect of NEUROG2 on the activity of different mutated versions of E940 in luciferase assays. The E940mut123 and E940mut3 are more sensitive to NEUROG2 repression than E940 or E940mut1 (E940, $n = 9$; E940mutRAR123, $n = 4$; E940RARmut1 $n = 3$; E940RARmut3, $n = 4$). P value < 0.05 *, P value < 0.01 **, Mann-Whitney test. **B.** Scheme presenting the strength of the repression of the different E940mutRAR forms and modeling the hypothesized changes in accessibility of the different RAREs following RAREs mutation. Green and blue bars represent the RAREs motifs, * indicates the mutated RAREs. In orange are NEUROG2 target proteins, in blue are RAR-RXRs heterodimers. REP in small upper case letters indicates normal repression, REP in large upper case letters indicates strong repression. **C.** Co-electroporation of pLac00E940-GFP (in green) with empty control vectors pADRSV and pCS2 (a, a'), pADRSVNEUROG2 and pCS2 (b, b'), pADRSV and pCS2RAR^{delAF2} (c, c'), pADNEUROG2 and pCS2RAR^{delAF2} (d, d'). H2bRFP was included in all conditions (in red). Embryos were electroporated at HH12 and harvested 18 h later. **D. Left panel:** Quantitative expression of E940-LUC when co-electroporated with the indicated constructs; **Right panel:** Fold change in E940-LUC expression upon the action of NEUROG2, RAR^{delAF2} or both as indicated at the bottom table. This is a complementary representation of the results presented in (a). **E.** The chicken HOMZ sequence is shown in the upper part with positions of arrayed putative NR binding sites (NRBS) indicated with arrows (note that they are all similarly oriented), the RAR::RXR cognate site being framed. Corresponding NRBS sequences are aligned below (positions within HOMZ are indicated on the right), with strictly conserved residues in white on a red background and partially conserved ones in red on a white background. A consensus LOGO sequence is shown beneath that is highly similar to the ZFC4-NR consensus sequence. **F. Schematic model proposed from our results:** NEUROG2 and RAR-RXR heterodimers act through the same DNA motif to oppositely control PAX6 temporal expression. This motif being enriched in putative nuclear receptor cognate sites and NRs being able to repress endogenous PAX6 and E940-GFP expression, we propose that NEUROG2 could activate a combination of NRs that would compete with RAR-RXR heterodimers for fixation on HOMZ.

even if it shows some activity in r5 at early stages. All these observations point to E940 being specifically dedicated to control PAX6^{ON/OFF} during the course of neurogenesis. This poses the question of whether this CRM is crucial for PAX6 expression or whether it acts redundantly with yet another unidentified neural enhancer. In a transgenic mouse study analyzing transcriptional activity in reporter yeast artificial chromosomes (YACs) containing large genomic sequences of the PAX6 locus, it was shown that YAC transgenes lacking

the downstream regulatory region (DRR) of PAX6 and containing E940, no longer showed proper GFP expression in the developing eye, emphasizing the importance of this remote control region in eye formation (Kleinjan et al., 2006). While the focus of that paper was on eye development, it was clear that removing the DRR from the YAC also leads to a strong reduction of reporter signal in the spinal cord. As E940 is a part of this DRR, the decrease in GFP expression in the neural tube upon removing the DRR could be due to missing E940

from the truncated YAC. However, some expression remained in the neural tube even in the absence of the DRR, suggesting the existence of some other neural tube enhancers in the genomic region present on the YAC but outside of the DRR. Genomic scanning of large regions surrounding the *PAX6* transcription units has in fact identified a large number of CRMs but only a few of them were able to drive robust neural tube activity. Two studies reported some *LACZ* expression in the spinal cord for an element (ELE4Q/ELE4H) located in the 4th intron of *PAX6* in quail, human and mouse, but its activity tested in the mouse was very caudal and late compared to endogenous *PAX6* expression (Plaza et al., 1995a; Xu and Saunders, 1998). Another enhancer located between the P0 and P1 *PAX6* promoters was reported to drive faint expression in the spinal cord (Kammandel et al., 1999). However these enhancers have not been functionally characterized in detail. More recently, Oosterveen et al., in a search for Gli-family binding sites in the vicinity of *SHH* target genes, identified a neural tube-specific enhancer GBS, located within the 7th intron of *PAX6*. This enhancer drives strong neural tube expression in the chick and is responsive to *SHH* signaling (Oosterveen et al., 2012), but we found that it is not downregulated by either *NEUROG2* or *dnRAR* overexpression, suggesting that it may be more specifically involved in the dorso-ventral restriction of *PAX6* expression. During the course of our study we also tested, another CRM, E55A, that was shown to drive strong reporter expression in the neural tube in transgenic mouse or zebrafish (Bhatia et al., 2014). We cloned the chick E55A, but it conferred only late expression of a *LACZ* reporter, and this expression was very weak, so we did not pursue further its characterization. Interestingly however, the ATAC-seq profile of E55A resembled that of E940: we detected significant peaks specifically in the neural tube and in r5 at E9.5. Therefore, E55A remains a promising CRM to be functionally dissected in the neural tube, and it could function redundantly with E940 in controlling *PAX6* temporal expression. Altogether these studies and our own data emphasize the complexity of *PAX6* regulation in a developing tissue such as the neural tube. They suggest that E940 is part of a CRM group dedicated to the control of *PAX6* expression in the neural tube and more specifically to the interpretation of temporal cues.

3.2. Antagonistic *NEUROG2* and *RA* signals act through a 60-bp-long motif within *HOMZ*

We showed that both positive and negative regulation of the E940 CRM by *RA* and *NEUROG2* act through a short 60 bp region within the *HOMZ* region. We identified 3 functional RAREs within E940, one being located in *HOMZ*. Mutation of these RAREs abolishes almost completely E940 activity in the neural tube, indicating that they are necessary for triggering positive *RA* response. The fact that E940mutRAR123 still responds partially to *RAR*-VP16 overexpression is possibly due to unspecific binding on DNA binding sites related to RAREs. During our *in silico* search for RAREs, we also found some putative *RXR*-VDR and *RXR*-THRB sites on E940. As DNA binding sites are highly similar between these different nuclear receptors, it is likely that in the absence of canonical RAREs, *RAR*-VP16, which is a strong constitutively active *RAR*, can bind to other putative binding sites and trigger some signal. However, we clearly demonstrate that RARE 1, 2, 3 are essential for E940 positive activity and interestingly, a single-base-pair mutation of RARE3, located in *HOMZ*, is sufficient to abolish positive activity while concomitantly increasing sensitivity to *NEUROG2*. As *NEUROG2* represses *PAX6* indirectly, this result favors a model in which the *NEUROG2* target gene(s) involved in *PAX6* repression and the positively acting *RAR*-*RXR*s heterodimers compete on shared cognate sites within *HOMZ*, and where the ratio between these two molecular players finely controls the balance of both spatial and temporal levels of *PAX6* in the developing neural tube.

A relationship between the retinoic acid pathway and *NEUROG2* has already been reported in the developing spinal cord. First, *NEUROG2* is activated by retinoic acid together with other neuronal

genes at the onset of neurogenesis (Novitsch et al., 2003; Diez del Corral et al., 2003; Ribes et al., 2008). Second, it has been shown that *RA* and *NEUROG2* cooperate for motoneuron (MN) specification (Lee et al., 2009). In this case, *RAR*-*NEUROG2* heterodimers are tethered on E-boxes and, upon fixation of *RA*, recruit CPB/p300 to regulate the expression of TFs involved in MN specification, such as *Hb9*. Our study brings to light a new mode of functional interaction between *RA* and *NEUROG2*, involving the sharing of a DNA motif to regulate target gene expression in opposing directions. Such a competitive interaction with *RA* signaling could be used more widely by *NEUROG2* as a way to efficiently repress other progenitors and/or cell cycle-controlling genes during the course of neurogenesis. In addition to *HOMZ*, we cannot exclude that another region in E940, the 5' part of E940, is also involved in *NEUROG2* repressive activity. We were unable to test that possibility because the fragment does not display any activity on its own, but when combined with a weak positive enhancer it led to a decrease in activity. Therefore, in addition to *HOMZ*, the 5' part of E940 could also carry a motif driving redundant negative activity.

3.3. *HOMZ* is enriched for predicted orphan nuclear receptor cognate sites

Our *in silico* analysis reveals a significant enrichment of putative nuclear receptor (NR) superfamily binding sites surrounding the *HOMZ* RARE, suggesting that several NRs could be involved in *PAX6* temporal regulation. Interestingly, such an involvement for nuclear receptors in temporal gene regulation has been described in *Drosophila* (Potier et al., 2014). Indeed, Potier et al. identified and validated NR binding sites located in a cardiac-specific enhancer acting in the adult fly. They showed that 3 distinct NRs behave as temporal transcriptional regulators acting through these heart enhancers. The NRs are relatives of *RORA*/B/C (*DHR3*) and *Rev-ErbB* (*E75A*/B/C) for which we found putative cognate sites within *HOMZ*. These NRs have been shown to interact physically with each other, allowing switching of *DHR3*-activating to repressive potential. It is tempting to propose a similar scenario in which *NEUROG2* activates or changes the activity of one or several NRs which then recruit other NR family partners or co-factors to form a repressive complex upon dedicated *HOMZ* sequences. This complex could exert a steric blockade on or around the RARE, impeding further binding of the *RAR*-*RXR* heterodimers. Alternatively, we can imagine that *NEUROG2* could change the stability or the activity of some particular NRs by activating genes involved in post-translational modification. NR function can be modulated by the recruitment of coactivators or repressor complexes (Auger and Jensen, 2009). It is thus also conceivable that *NEUROG2* induces the expression of NR co-factors that could change the activity or composition of NRs containing complexes leading to a repressive action. Identification of the NR target genes of *NEUROG2* and/or the co-factors known to functionally collaborate with NRs will be essential to allow further testing of that model.

4. Materials and methods

4.1. Ethics statement

All zebrafishes were handled in a facility certified by the French Ministry of Agriculture (approval ID B-31-555-10) and in accordance with the guidelines from the European directive on the protection of animals used for scientific purposes (2010/63/UE), French Decret 2013-118.

4.2. Zebrafish experiments

Zebrafish embryos were raised and staged as described in (Westerfield, 1995) and provided by P.Blader. The *ngn1*^{hi1059} line was generated by insertion of a mouse retroviral vector in the 3' UTR of

the *ngn1* gene (Golling et al., 2002). The thermo-sensitive *ngn1* transgenic line (Tg(hsp70I:neurog1:ups1)) was generated by inserting a transgene containing *ngn1* fused to a hsp70 heat shock inducible promoter (Madelaine and Blader, 2011). Heat shock was performed as follows: Embryos were raised in a 28 °C water bath, then transferred at the 21hpf (hour post fertilization) stage to a 38 °C water bath for one hour. Then they were replaced in a 28 °C water bath for 2 more hours before being fixed for in situ hybridization (ISH). Whole-mount ISH was performed as described in (Madelaine and Blader, 2011). Antisense riboprobes to detect *pax6b* and *DeltaD* transcripts were a gift from P.Blader. After ISH, embryos were embedded in gelatine/albumin and 10–15 µm sections were cut using a vibratome (Leica VT1000s).

4.3. Chicken embryos

Fertile hen's eggs (from *G. Gallus*) were provided by a local supplier (SCAL) and incubated at 37 °C in a humidified incubator for the appropriate time to reach the required Hamburger and Hamilton (HH) stage. Eggs were grown until HH10–HH12 (E1.5–2) to perform electric pulses. After electroporation, eggs were further incubated either 7 h, 18 h to 22 h or 36 h before harvesting.

4.4. Electroporation of DNA

Electroporation was performed as described on the left side of the neural tube. 0.5 to 3 µg/µl of DNA were injected in the lumen of the neural tube before applying 5 pulses of 20mv using square electrodes. The pADRSV-NEUROG2 flag and pADRSV constructs were a gift from P.Charnay (Garcia-Dominguez et al., 2003). The *Xenopus* dnRARα expressing construct was a gift from Nancy Papalopulu. It is a truncated *xenopus* RARα form that lacks amino acids 406 to 474, corresponding to the AF2 domain (xRARα1405*, (Blumberg et al., 1997)). H2b-RFP came from (Megason, 2009). RARdelAF2 is a human RAR alpha receptor truncated from the 374 amino acid, lacking part of the heterodimerisation domain and the AF2 domain (Lee et al., 2009). The pCAAG-RARα was from Addgene (clone 16287). The LAC00 vector in which the CRMs were first cloned was given by J.M. Matter (Crossley and Brownlee, 1990; Hernandez et al., 1995). The d2EGFP vectors were derived from the pCIG plasmid (Megason and McMahon, 2002). For luciferase assays, all the tested CRMs were cloned into a pGL4.23 [luc2/minP] vector (Promega), and in some cases the PAX3CNE1 enhancer (E^{min}) (Moore et al., 2013) was also inserted into this vector. The HM mutated forms HM1 to HM8 were generated by PCR, using the overlap extension method (Ho et al., 1989). Every 10 bp on HOMZ were replaced by a NOT1 site flanked by two additional base pairs (GGGGGGCGCCGCC).

4.5. Production and analysis of reporter transgenic mice

The mE940 construct was made by PCR amplification of a 1.54 kb fragment (hg38 assembly chr11:31650121–31651659) with primer pair: 5'-TGCTTTTCCTTGTGACACT-3' and 5'-TCATATACGGCAGATTCCTCG-3', cloned into pGEM-T (Promega), followed by subcloning into the NotI site of the p610+LacZ reporter vector. Microinjection fragments were generated by digestion with suitable restriction enzymes, isolated from agarose gel using Qiagen gel extraction columns and microinjected into mouse oocytes according to standard procedures. Transgenic mice and embryos were identified by PCR using LacZ specific primers. A number of transient transgenic embryos and two expressing lines were obtained, showing a sub-pattern of the previously characterized HS5 +/Z transgenic expression pattern (McBride et al., 2011).

4.6. In situ hybridization, Immunohistochemistry and LACZ staining

Detection of transcripts and protein was done on 50 µm thick transversal sections (made with a vibratome) that were embedded in

5% agarose following 3 h fixation in 4% paraformaldehyde at RT. *In situ* hybridization was performed as published in (Bel-Vialar et al., 2002). Riboprobes to detect PAX6 transcripts were synthesized from isolated specific PCR products devoid of plasmid sequences to avoid unspecific cross reaction between the riboprobe and electroporated plasmids (oligonucleotides are available on request).

Immunohistochemistry was performed as described in (Lobjois et al., 2004). The antibodies we used were as follows: a monoclonal anti-human neuronal protein HuC/HuD (anti-HuC/D; Molecular Probes; 1/500); a polyclonal rabbit anti-PAX6 (Covance, ref. PRB-278P, 1/300); a polyclonal anti-Ngn2 (from D. Anderson; 1/3000). LACZ staining was done as described in (Bel-Vialar et al., 2002).

4.7. Dual luciferase assay

The luciferase assays were performed with the Dual Luciferase reporter assay kit (Promega), according to the manufacturer's recommendations. The different forms of E940, cloned into the pGL4.23 firefly vector, were electroporated into E1.5–2 neural tubes at a concentration close to 0.5 µg/µl. The concentration of the empty pGL4.23 firefly vector was 0.5 µg/µl and all E940 forms or subfragment concentrations were calculated depending of their length in order to obtain the same final number of molecules. Each test also included a pGL3 Renilla vector at 0.05 µg/µl that served to normalize the firefly measure with the quantity of electroporated cells. NEUROG2, NEUROG2AQ, dnRARα and RAR^{delAF2} were electroporated at a concentration of 0.5 µg/µl. Neural tubes were collected 18 h following electroporation and lysed in the provided lysis buffer before measuring luciferase activity. At least three neural tubes were pooled for each experimental condition, and all experiments were reproduced at least three times. All the results are expressed as a mean ± SEM of at least three independent experiments, and statistical significance was evaluated when relevant using the Mann-Whitney test.

4.8. Confocal analysis

Confocal images were acquired on a SP8 Leica confocal microscope from optical slices of 4µm depth with an x40 objective.

4.9. Bioinformatics

Genomic sequences homologous to chicken E940 were recovered through BLAST analyses at NCBI (<https://blast.ncbi.nlm.nih.gov/Blast.cgi>). Multiple sequence alignments were generated with MAFFT version 7.0 (<http://mafft.cbrc.jp/alignment/server/>) and colored with ESPript version 3.0 (<http://esprict.ibcp.fr/ESPript/ESPript/>) using the Risler homology matrix (global score of 0.7). Putative RARES sites were identified using the Mat Inspector module of the genomatrix software suite (<https://www.genomatrix.de>). Clustered putative NR binding sites within HOMZ were identified through the MEME suite version 4.11.4 (<http://meme-suite.org/index.html>) as well as through visual inspection, and the corresponding consensus sequence was generated with WebLogo (<http://weblogo.berkeley.edu/logo.cgi>).

4.10. ATAC-seq experiments (Thierion et al., 2017)

ATAC experiments were performed according to Buenrostro and colleagues (Buenrostro et al., 2013), using a homemade transposome (Picelli et al., 2014). For each genotype, 7–8 embryos at 10–12 s were dissected in cold PBS and cells were mechanically dissociated. Cells were lysed before transposition using 1 µl of transposome and purified using a Qiagen MinElute Kit with 10 µl of Elution Buffer. Transposed DNA was amplified by PCR as previously described (Buenrostro et al., 2013) and quantified by qPCR using 5 µl of PCR product. The number of additional cycles was determined by plotting linear Rn versus cycle and corresponded to one third of the maximum fluorescence intensity. The

remaining PCR product (45 µl) was treated with the additional number of cycles. The final product was purified with Qiagen PCR Cleanup Kit and eluted in 20 µl Elution Buffer. Sequencing was performed on multiplexed samples using 42 bp paired-end reads on an Illumina NextSeq according to the manufacturer's specifications. For computational analysis, paired-end reads were mapped onto the mouse genome assembly mm9 using STAR (outFilterMultimapNmax 1; outFilterMismatchNmax 999; outFilterMismatchNoverLmax 0.06; alignIntronMax 1; alignEndsType EndToEnd; alignMatesGapMax 2000). Duplicate reads were removed using Picard (<http://picard.sourceforge.net>) (MarkDuplicates, REMOVE_DUPLICATES = true). To consider only those fragments coming from transcription factor protected DNA (and not from nucleosomes), only fragments smaller than 100 bp were kept. BIGWIG tracks were obtained using DeepTools BamCoverage (1.5.9.1).

4.11. ChIP-seq experiments (Thierion et al., 2017)

ChIP-seq experiments were performed as previously described (Vitobello et al., 2011). Briefly, 10 embryos at E9.5 were dissected in cold PBS. Cell suspensions were obtained by passage through a 21 G needle fitted onto a 5 ml syringe. The cells were cross-linked with 1% formaldehyde for 10 min and washed twice in PBS, 1 mM PMSF, 1 × PIC (Protease Inhibitor Cocktail). Sonication was performed on a Covaris S220 using the following programme: duty factor = 10, peak incident power = 140, cycles per burst = 200 during 600 seconds. 10 µg of chromatin were used for each IP using 3 µg of the following antibodies: anti H3K4me1 (C15410037, Diagenode) and anti H3K27ac (ab4729, Abcam) in RIPA buffer. The libraries were prepared with the MicroPlex Library Preparation kit (Diagenode, E8.5 embryos) and with the NEXTflex ChIP-Seq Kit (Bioo Scientific, E9.5 embryos). ChIP Seq experiments were done in duplicate.

Sequencing was performed on multiplexed samples using 50 bp single-end reads on an Illumina HiSeq system (E9.5 embryos), or using 42 bp paired-end reads on an Illumina NextSeq (E8.5 embryos) according to the manufacturer's specifications. Chip-seq data were analysed, using Eoulsan (Jourden et al., 2012) with extended support for ChIP-seq workflows (<https://github.com/GenomicParisCentre/eoulsan/tree/branch-chip-seq>), see (Thierion et al., 2017). Mapping was performed using STAR (Dobin et al., 2013) (version 2.4.0k in module mapreads). Further filters were applied to the mapped reads before conversion into BAM, (Thierion et al., 2017). BIGWIG files were created from the resulting BAM files using deepTools' bamCoverage (Ramirez et al., 2014). The ATAC-seq and ChIP-seq data have been deposited in the Gene Expression Omnibus (GEO) under accession number GSE94716 (Thierion et al., 2017).

4.12. Genomic sequences

The coordinates for the genomic sequences used in this study are: Chicken E940: Galgal4:5:5141000:5142000:1; Human E940: GRCh38:11:31650584:31651473:1; Mouse E940: GRCm38:2:105790983:105791885:1; Mouse HS5 +: GRCm38-2:105790856-105793087.1(-); Mouse HOMZ: GRCm38:2:105791242-105791346; Zebrafish HOMZ:GRCz10:25:14870614-14870716; Mouse GBS: GRCm38:2:105689932-105690425; Mouse E55A: GRCm38:2:105610856-105611811.

Acknowledgments

We thank Patrick Blader and Pascale Dufourcq for providing zebrafish embryos and expertise. We thank Alice Baldy, Alicia Malet and the Imagery Platform TRI Toulouse for technical support. We also thank members of our team, members of Alice Davy's team, Michelle Studer and Vanessa Ribes for helpful discussions. Finally we thank Pascale Gilardi-Hebenstreit, Serge Plaza and Muriel Boube for critical reading of the manuscript.

Funding

This work was supported by grants for ML from the CNRS and region Midi-Pyrenees. Core support was from the CNRS and University Paul Sabatier, Toulouse. The funders had no role in study design, data collection and analysis, decision to publish, or preparation of the manuscript.

Appendix A. Supporting information

Supplementary data associated with this article can be found in the online version at doi:10.1016/j.ydbio.2018.02.015.

References

- Auger, A.P., Jessen, H.M., 2009. Corepressors, nuclear receptors, and epigenetic factors on DNA: a tail of repression. *Psychoneuroendocrinology* 34 (Suppl 1), S39–S47.
- Bel-Vialar, S., Itasaki, N., Krumlauf, R., 2002. Initiating Hox gene expression: in the early chick neural tube differential sensitivity to FGF and RA signaling subdivides the HoxB genes in two distinct groups. *Development* 129, 5103–5115.
- Bel-Vialar, S., Medevielle, F., Pituello, F., 2007. The on/off of Pax6 controls the tempo of neuronal differentiation in the developing spinal cord. *Dev. Biol.* 305, 659–673.
- Bertrand, N., Castro, D.S., Guillemot, F., 2002. Proneural genes and the specification of neural cell types. *Nat. Rev. Neurosci.* 3, 517–530.
- Bertrand, N., Medevielle, F., Pituello, F., 2000. FGF signalling controls the timing of Pax6 activation in the neural tube. *Development* 127, 4837–4843.
- Bhatia, S., Monahan, J., Ravi, V., Gautier, P., Murdoch, E., Brenner, S., van Heyningen, V., Venkatesh, B., Kleinjan, D.A., 2014. A survey of ancient conserved non-coding elements in the PAX6 locus reveals a landscape of interdigitated cis-regulatory archipelagos. *Dev. Biol.* 387, 214–228.
- Blader, P., Fischer, N., Gradwohl, G., Guillemot, F., Strahle, U., 1997. The activity of neurogenin1 is controlled by local cues in the zebrafish embryo. *Development* 124, 4557–4569.
- Blumberg, B., Bolado, J., Moreno, T., Kintner, C., Evans, R., Papalopulu, N., 1997. An essential role for retinoid signaling in anteroposterior neural patterning. *Development* 124, 373–379.
- Buenrostro, J.D., Giresi, P.G., Zaba, L.C., Chang, H.Y., Greenleaf, W.J., 2013. Transposition of native chromatin for fast and sensitive epigenomic profiling of open chromatin, DNA-binding proteins and nucleosome position. *Nat. Methods* 10, 1213–1218.
- Cartharius, K., Frech, K., Grote, K., Klocke, B., Haltmeier, M., Klingenhoff, A., Frisch, M., Bayerlein, M., Werner, T., 2005. MatInspector and beyond: promoter analysis based on transcription factor binding sites. *Bioinformatics* 21, 2933–2942.
- Chitnis, A., Henrique, D., Lewis, J., Ish-Horowitz, D., Kintner, C., 1995. Primary neurogenesis in *Xenopus* embryos regulated by a homologue of the *Drosophila* neurogenic gene Delta. *Nature* 375, 761–766.
- Crossley, M., Brownlee, G.G., 1990. Disruption of a C/EBP binding site in the factor IX promoter is associated with haemophilia B. *Nature* 345, 444–446.
- Cvekl, A., Callaerts, P., 2016. PAX6: 25th anniversary and more to learn. *Exp. Eye Res.*
- Diez del Corral, R., Olivera-Martinez, I., Goriely, A., Gale, E., Maden, M., Storey, K., 2003. Opposing FGF and retinoid pathways control ventral neural pattern, neuronal differentiation, and segmentation during body axis extension. *Neuron* 40, 65–79.
- Dixit, R., Wilkinson, G., Cancino, G.I., Shaker, T., Adnani, L., Li, S., Dennis, D., Kurrasch, D., Chan, J.A., Olson, E.C., Kaplan, D.R., Zimmer, C., Schuurmans, C., 2014. Neurog1 and Neurog2 control two waves of neuronal differentiation in the piriform cortex. *J. Neurosci.* 34, 539–553.
- Dobin, A., Davis, C.A., Schlesinger, F., Drenkow, J., Zaleski, C., Jha, S., Batut, P., Chaisson, M., Gingeras, T.R., 2013. STAR: ultrafast universal RNA-seq aligner. *Bioinformatics* 29, 15–21.
- Ericson, J., Rashbass, P., Schedl, A., Brenner-Morton, S., Kawakami, A., van Heyningen, V., Jessell, T.M., Briscoe, J., 1997. Pax6 controls progenitor cell identity and neuronal fate in response to graded Shh signaling. *Cell* 90, 169–180.
- Garcia-Dominguez, M., Poquet, C., Garel, S., Charnay, P., 2003. Ebf gene function is required for coupling neuronal differentiation and cell cycle exit. *Development* 130, 6013–6025.
- Ge, W., He, F., Kim, K.J., Blanchi, B., Coskun, V., Nguyen, L., Wu, X., Zhao, J., Heng, J.I., Martinovich, K., Tao, J., Wu, H., Castro, D., Sobeih, M.M., Corfas, G., Gleeson, J.G., Greenberg, M.E., Guillemot, F., Sun, Y.E., 2006. Coupling of cell migration with neurogenesis by proneural bHLH factors. *Proc. Natl. Acad. Sci. USA* 103, 1319–1324.
- Golling, G., Amsterdam, A., Sun, Z., Antonelli, M., Maldonado, E., Chen, W., Burgess, S., Haldi, M., Artzt, K., Farrington, S., Lin, S.Y., Nissen, R.M., Hopkins, N., 2002. Insertional mutagenesis in zebrafish rapidly identifies genes essential for early vertebrate development. *Nat. Genet.* 31, 135–140.
- Griffin, C., Kleinjan, D.A., Doe, B., van Heyningen, V., 2002. New 3' elements control Pax6 expression in the developing pretectum, neural retina and olfactory region. *Mech. Dev.* 112, 89–100.
- Hernandez, M.C., Erkman, L., Matter-Sadzinski, L., Roztocil, T., Ballivet, M., Matter, J.M., 1995. Characterization of the nicotinic acetylcholine receptor beta 3 gene. Its regulation within the avian nervous system is effected by a promoter 143 base pairs in length. *J. Biol. Chem.* 270, 3224–3233.

- Ho, S.N., Hunt, H.D., Horton, R.M., Pullen, J.K., Pease, L.R., 1989. Site-directed mutagenesis by overlap extension using the polymerase chain reaction. *Gene* 77, 51–59.
- Itasaki, N., Bel-Vialar, S., Krumlauf, R., 1999. "Shocking" developments in chick embryology: electroporation and *in ovo* gene expression. *Nat. Cell Biol.* 1, E203–E207.
- Janesick, A., Wu, S.C., Blumberg, B., 2015. Retinoic acid signaling and neuronal differentiation. *Cell. Mol. Life Sci.* 72, 1559–1576.
- Jourdren, L., Bernard, M., Dillies, M.A., Le Crom, S., 2012. Eoulsan: a cloud computing-based framework facilitating high throughput sequencing analyses. *Bioinformatics* 28, 1542–1543.
- Kammandel, B., Chowdhury, K., Stoykova, A., Aparicio, S., Brenner, S., Gruss, P., 1999. Distinct cis-essential modules direct the time-space pattern of the Pax6 gene activity. *Dev. Biol.* 205, 79–97.
- Kayam, G., Kohl, A., Magen, Z., Peretz, Y., Weisinger, K., Bar, A., Novikov, O., Brodski, C., Sela-Donnenfeld, D., 2013. A novel role for Pax6 in the segmental organization of the hindbrain. *Development* 140, 2190–2202.
- Kim, J., Lauderdale, J.D., 2006. Analysis of Pax6 expression using a BAC transgene reveals the presence of a paired-less isoform of Pax6 in the eye and olfactory bulb. *Dev. Biol.* 292, 486–505.
- Kleinjan, D., Seawright, A., Child, A., van heynigen, V., 2004. Conserved elements in Pax6 intron 7 involved in (auto)regulation and alternative transcription. *Dev. Biol.* 265, 462–477.
- Kleinjan, D.A., Bancewicz, R.M., Gautier, P., Dahm, R., Schonthal, H.B., Damante, G., Seawright, A., Hever, A.M., Yeyati, P.L., van Heyningen, V., Coutinho, P., 2008. Subfunctionalization of duplicated zebrafish pax6 genes by cis-regulatory divergence. *PLoS Genet.* 4, e29.
- Kleinjan, D.A., Seawright, A., Mella, S., Carr, C.B., Tyas, D.A., Simpson, T.I., Mason, J.O., Price, D.J., van Heyningen, V., 2006. Long-range downstream enhancers are essential for Pax6 expression. *Dev. Biol.* 299, 563–581.
- Kleinjan, D.A., Seawright, A., Schedl, A., Quinlan, R.A., Danes, S., van Heyningen, V., 2001. Aniridia-associated translocations, DNase hypersensitivity, sequence comparison and transgenic analysis redefine the functional domain of PAX6. *Hum. Mol. Genet.* 10, 2049–2059.
- Kleinjan, D.A., van Heyningen, V., 2005. Long-range control of gene expression: emerging mechanisms and disruption in disease. *Am. J. Hum. Genet.* 76, 8–32.
- Kovach, C., Dixit, R., Li, S., Mattar, P., Wilkinson, G., Elsen, G.E., Kurrasch, D.M., Hevner, R.F., Schuurmans, C., 2013. Neurog2 simultaneously activates and represses alternative gene expression programs in the developing neocortex. *Cereb. Cortex* 23, 1884–1900.
- Lacomme, M., Liaubet, L., Pituello, F., Bel-Vialar, S., 2012. NEUROG2 drives cell cycle exit of neuronal precursors by specifically repressing a subset of cyclins acting at the G1 and S phases of the cell cycle. *Mol. Cell Biol.* 32, 2596–2607.
- Lee, S., Lee, B., Lee, J.W., Lee, S.K., 2009. Retinoid signaling and neurogenin2 function are coupled for the specification of spinal motor neurons through a chromatin modifier CBP. *Neuron* 62, 641–654.
- Lobjois, V., Benazeraf, B., Bertrand, N., Medevielle, F., Pituello, F., 2004. Specific regulation of cyclins D1 and D2 by FGF and Shh signaling coordinates cell cycle progression, patterning, and differentiation during early steps of spinal cord development. *Dev. Biol.* 273, 195–209.
- Ma, Q., Chen, Z., del Barco Barrantes, I., de la Pompa, J.L., Anderson, D.J., 1998. neurogenin1 is essential for the determination of neuronal precursors for proximal cranial sensory ganglia. *Neuron* 20, 469–482.
- Ma, Q., Kintner, C., Anderson, D.J., 1996. Identification of neurogenin, a vertebrate neuronal determination gene. *Cell* 87, 43–52.
- Madelaine, R., Blader, P., 2011. A cluster of non-redundant Ngn1 binding sites is required for regulation of deltaA expression in zebrafish. *Dev. Biol.* 350, 198–207.
- Mangelsdorf, D.J., Evans, R.M., 1995. The RXR heterodimers and orphan receptors. *Cell* 83, 841–850.
- McBride, D.J., Buckle, A., van Heyningen, V., Kleinjan, D.A., 2011. DNaseI hypersensitivity and ultraconservation reveal novel, interdependent long-range enhancers at the complex Pax6 cis-regulatory region. *PLoS One* 6, e28616.
- Megason, S.G., 2009. In toto imaging of embryogenesis with confocal time-lapse microscopy. *Methods Mol. Biol.* 546, 317–332.
- Megason, S.G., McMahon, A.P., 2002. A mitogen gradient of dorsal midline Wnts organizes growth in the CNS. *Development* 129, 2087–2098.
- Moore, S., Ribes, V., Terriente, J., Wilkinson, D., Relaix, F., Briscoe, J., 2013. Distinct regulatory mechanisms act to establish and maintain Pax3 expression in the developing neural tube. *PLoS Genet.* 9, e1003811.
- Nornes, S., Clarkson, M., Mikkola, I., Pedersen, M., Bardsley, A., Martinez, J.P., Krauss, S., Johansen, T., 1998. Zebrafish contains two pax6 genes involved in eye development. *Mech. Dev.* 77, 185–196.
- Novitsch, B.G., Wichterle, H., Jessell, T.M., Sockanathan, S., 2003. A requirement for retinoic acid-mediated transcriptional activation in ventral neural patterning and motor neuron specification. *Neuron* 40, 81–95.
- Oosterveen, T., Kurdija, S., Alekseenko, Z., Uhde, C.W., Bergsland, M., Sandberg, M., Andersson, E., Dias, J.M., Muhr, J., Ericson, J., 2012. Mechanistic differences in the transcriptional interpretation of local and long-range Shh morphogen signaling. *Dev. Cell* 23, 1006–1019.
- Osumi, N., Shinohara, H., Numayama-Tsuruta, K., Maekawa, M., 2008. Concise review: Pax6 transcription factor contributes to both embryonic and adult neurogenesis as a multifunctional regulator. *Stem Cells* 26, 1663–1672.
- Picelli, S., Bjorklund, A.K., Reinis, B., Sagasser, S., Winberg, G., Sandberg, R., 2014. Tn5 transposase and tagmentation procedures for massively scaled sequencing projects. *Genome Res.* 24, 2033–2040.
- Pituello, F., 1997. Neuronal specification: generating diversity in the spinal cord. *Curr. Biol.* 7, R701–R704.
- Plaza, S., Dozier, C., Langlois, M.C., Saule, S., 1995a. Identification and characterization of a neuroretina-specific enhancer element in the quail Pax-6 (Pax-QNR) gene. *Mol. Cell Biol.* 15, 892–903.
- Plaza, S., Dozier, C., Turque, N., Saule, S., 1995b. Quail Pax-6 (Pax-QNR) mRNAs are expressed from two promoters used differentially during retina development and neuronal differentiation. *Mol. Cell Biol.* 15, 3344–3353.
- Potier, D., Seyres, D., Guichard, C., Iche-Torres, M., Aerts, S., Herrmann, C., Perrin, L., 2014. Identification of cis-regulatory modules encoding temporal dynamics during development. *BMC Genom.* 15, 534.
- Ramirez, F., Dundar, F., Diehl, S., Gruning, B.A., Manke, T., 2014. deepTools: a flexible platform for exploring deep-sequencing data. *Nucleic Acids Res.* 42, W187–W191.
- Ribes, V., Stutzmann, F., Bianchetti, L., Guillemot, F., Dolle, P., Le Roux, I., 2008. Combinatorial signalling controls Neurogenin2 expression at the onset of spinal neurogenesis. *Dev. Biol.* 321, 470–481.
- Ross, S.E., Greenberg, M.E., Stiles, C.D., 2003. Basic helix-loop-helix factors in cortical development. *Neuron* 39, 13–25.
- Sansom, S.N., Griffiths, D.S., Faedo, A., Kleinjan, D.J., Ruan, Y., Smith, J., van Heyningen, V., Rubenstein, J.L., Livesey, F.J., 2009. The level of the transcription factor Pax6 is essential for controlling the balance between neural stem cell self-renewal and neurogenesis. *PLoS Genet.* 5, e1000511.
- Simpson, T.I., Price, D.J., 2002. Pax6; a pleiotropic player in development. *Bioessays* 24, 1041–1051.
- Spitz, F., Furlong, E.E., 2012. Transcription factors: from enhancer binding to developmental control. *Nat. Rev. Genet.* 13, 613–626.
- St-Onge, L., Sosa-Pineda, B., Chowdhury, K., Mansouri, A., Gruss, P., 1997. Pax6 is required for differentiation of glucagon-producing alpha-cells in mouse pancreas. *Nature* 387, 406–409.
- Sun, Y., Nadal-Vicens, M., Misono, S., Lin, M.Z., Zubiaga, A., Hua, X., Fan, G., Greenberg, M.E., 2001. Neurogenin promotes neurogenesis and inhibits glial differentiation by independent mechanisms. *Cell* 104, 365–376.
- Thierion, E., Le Men, J., Collombet, S., Hernandez, C., Couplier, F., Torbey, P., Thomas-Chollier, M., Noordermeer, D., Charnay, P., Gilardi-Hebenstreit, P., 2017. Krox20 hindbrain regulation incorporates multiple modes of cooperation between cis-acting elements. *PLoS Genet.* 13, e1006903.
- Umesono, K., Murakami, K.K., Thompson, C.C., Evans, R.M., 1991. Direct repeats as selective response elements for the thyroid hormone, retinoic acid, and vitamin D3 receptors. *Cell* 65, 1255–1266.
- van Heyningen, V., Williamson, K.A., 2002. PAX6 in sensory development. *Hum. Mol. Genet.* 11, 1161–1167.
- Vitobello, A., Ferretti, E., Lampe, X., Vilain, N., Ducret, S., Ori, M., Spetz, J.F., Selleri, L., Rijli, F.M., 2011. Hox and Pbx factors control retinoic acid synthesis during hindbrain segmentation. *Dev. Cell* 20, 469–482.
- Westerfield, M. (Ed.), 1995. A Guide for the Laboratory Use of Zebrafish (*Danio rerio*). OR: University of Oregon Press, Eugene.
- Williams, S.C., Altmann, C.R., Chow, R.L., Hemmati-Brivanlou, A., Lang, R.A., 1998. A highly conserved lens transcriptional control element from the Pax-6 gene. *Mech. Dev.* 73, 225–229.
- Xu, P.X., Zhang, X., Heaney, S., Yoon, A., Michelson, A.M., Maas, R.L., 1999. Regulation of Pax6 expression is conserved between mice and flies. *Development* 126, 383–395.
- Xu, Z.P., Saunders, G.F., 1998. PAX6 intronic sequence targets expression to the spinal cord. *Dev. Genet.* 23, 259–263.
- Zhou, V.W., Goren, A., Bernstein, B.E., 2011. Charting histone modifications and the functional organization of mammalian genomes. *Nat. Rev. Genet.* 12, 7–18.